© 2026 International Conference on Multidisciplinary Sciences and Innovations . All Rights Reserved.

EFFECT OF STEAM ACTIVATION TEMPERATURE ON THE PORE STRUCTURE OF SHARGUN COAL (SURKHANDARYA, UZBEKISTAN): COMPARISON OF THE 600 AND 850 °C REGIMES

S. M. Isayev, A. M. Qudratov
Shift engineer, ACWA Operation Company, Chirchiq, Uzbekistan
e-mail: Sobirjon8698@gmail.com ORCID: 0009-0001-4396-8455
Professor, Department of Artificial Intelligence and Natural Sciences,
University of Geological Sciences, Tashkent, Uzbekistan
e-mail: prof-akmaljon@mail.ru

Abstract. Uzbekistan imports almost all of the activated carbon used in industrial water treatment, and coal from the Shargun deposit is an obvious candidate feedstock. An earlier stage of this work established that the raw coal has no micropore network accessible to nitrogen and a surface area of only 12.142 m^2/g, so its value as an adsorbent depends entirely on activation. Here the governing parameter of that step — temperature — is examined by comparing two regimes, 600 and 850 °C, each consisting of one hour of pyrolysis followed by one hour of steam activation in the same laboratory rig. Pore structure was determined by nitrogen physisorption at 77.35 K and morphology and composition by SEM–EDS. At 600 °C no micropore network formed: the surface area did not exceed the feedstock value and the modal half-width moved from 2.59 to 7.66 nm, that is, existing pores merely widened. At 850 °C a microporous structure appeared: the surface area reached 33.704 m^2/g, the modal half-width fell to 1.66 nm, and uptake at a relative pressure of 0.053 was 7.94 cm^3/g against 0.167 for the raw coal, a factor of 47.5. Over the common width range 0.74–5.53 nm the activated sample exceeds the feedstock by 1.67 times in pore volume and by 6.7 times in surface area. The BET equation failed for both samples but for opposite reasons: C = 1.799 for the raw coal and C = −36.725 for AC-850. The working regime should therefore be built around 850 °C, and the reported surface area is a lower bound, since the micropore filling region was not sampled.

Keywords: Shargun coal; steam activation; activation temperature; micropores; QSDFT; BET; SEM–EDS; import substitution.

1. Introduction

Hydrogen production units and high-pressure steam boilers operate only on deeply purified water, and the activated carbon filter is a small but non-substitutable element of every water-treatment train: it removes residual chlorine, protecting reverse-osmosis membranes, and retains dissolved organic matter [3, 4]. The national programmes set out in Presidential Resolution PQ-5063 [1] and in the Uzbekistan – 2030 Strategy [2] will raise industrial demand for such water sharply, yet almost all of the activated carbon used in the country is imported. Domestic experience exists for agricultural residues — an import-substituting carbon has been obtained from plum stones by steam activation [5] — but mineral feedstock has scarcely been examined.

Our earlier measurements on coal from the Shargun deposit showed that the raw material contains no micropore network accessible to nitrogen and that its surface area does not exceed 12.142 m2/g. Its value as an adsorbent is therefore created entirely in the activation step, whose principal control parameter is temperature. The reaction of carbon with steam is endothermic and has a high activation energy, so its rate depends steeply on temperature [6, 7]; and the texture of the parent material also governs the outcome, which means that a regime established for one feedstock cannot simply be transferred to another [8]. For Shargun coal no such regime has been published. The aim of this work is to compare the 600 and 850 °C regimes and to locate the temperature region in which a microporous structure actually forms.

© 2026 International Conference on Multidisciplinary Sciences and Innovations . All Rights Reserved.

2. Materials and methods

2.1. Activation. Crushed and air-dried Shargun coal was processed in a laboratory rig comprising a horizontal tubular pyrolysis furnace with a resistance heating coil, a PID controller with a thermocouple placed next to the sample inside the reactor, a steam generator with a sight glass and pressure gauge, and an off-gas line. The steam line runs along the furnace body so that the steam is superheated before it enters the reaction zone, which prevents droplets from reaching the sample and cooling it locally. The sample was placed in a boat in the isothermal zone, the tube was sealed, and the furnace was heated to the set point with the steam valve closed. Pyrolysis was then carried out for one hour; the steam valve was opened without changing the temperature and activation continued for a further hour, the carbon reacting as $C + H_2O \rightarrow CO + H_2$, with the water–gas shift proceeding in parallel. Two regimes were run, at 600 and at 850 °C, with pyrolysis time, activation time, steam supply and sample mass held constant; the samples are designated AC-600 and AC-850.

2.2. Characterisation. Pore structure was measured on a Quantachrome Autosorb iQ with ASiQwin 5.21, using nitrogen at 77.35 K; the void volume was measured with helium and a thermal transpiration correction was applied. Morphology was observed on a JEOL JSM-IT210 scanning electron microscope and spot composition on its energy-dispersive spectrometer at 20 kV with standardless ZAF correction. Sample and measurement details are given in Table 1.

Table 1 – Samples, activation regimes and conditions of the sorption measurement

Parameter	**Raw coal**	**AC-600**	**AC-850**
Preparation	as received	600 °C; 1 h pyrolysis + 1 h steam	850 °C; 1 h pyrolysis + 1 h steam
Sample mass, g	0.1502	0.2070	0.2218
Outgassing	200 °C, 1.3 h	110 °C, 0.5 h	200 °C, 1.3 h
DFT kernel	QSDFT (slit/cyl.)	NLDFT (slit)	QSDFT (slit/cyl.)
Cold-zone volume, cm3	1.53141	1.50860	2.33515
Total surface in cell, m2	1.82	1.40	7.48

2.3. Limits of the comparison. Three constraints follow from Table 1 and are applied throughout. First, AC-600 was outgassed under a milder regime and processed with a different kernel, so its figures are treated as a lower bound and are not compared numerically with the other two. Second, the three samples were processed over different pore-width ranges, so the "total" values of Table 2 are not mutually comparable; a common-range comparison is given separately in Table 3. Third, the total surface present in the measuring cell — the last line of Table 1 — was 1.82 and 1.40 m^2 for the raw coal and AC-600, below the 5–10 m^2 normally recommended for nitrogen at 77 K, and 7.48 m^2 for AC-850. The decisive measurement of this study is thus also the most reliable one.

3. Results

3.1. Isotherms. The three isotherms (Figure 1) differ in kind, not in degree. Those of the raw coal and of AC-600 are convex to the relative-pressure axis over their whole length and show no point B; uptake rises steeply only above $P/P_0 = 0.95$. They are therefore close to IUPAC Type III rather than Type II, which for the raw coal is confirmed numerically by its BET constant of 1.799, since $C < 2$ corresponds to Type III within BET theory. The AC-850 isotherm is of Type I: uptake is already 7.94 cm^3/g at $P/P_0 = 0.053$ and reaches 8.43 cm^3/g by 0.15. Against 0.167 cm^3/g for the raw

© 2026 International Conference on Multidisciplinary Sciences and Innovations . All Rights Reserved.

coal at the same relative pressure this is a factor of 47.5, and it can only arise from micropores, since meso- and macropores do not fill appreciably at such low pressure.

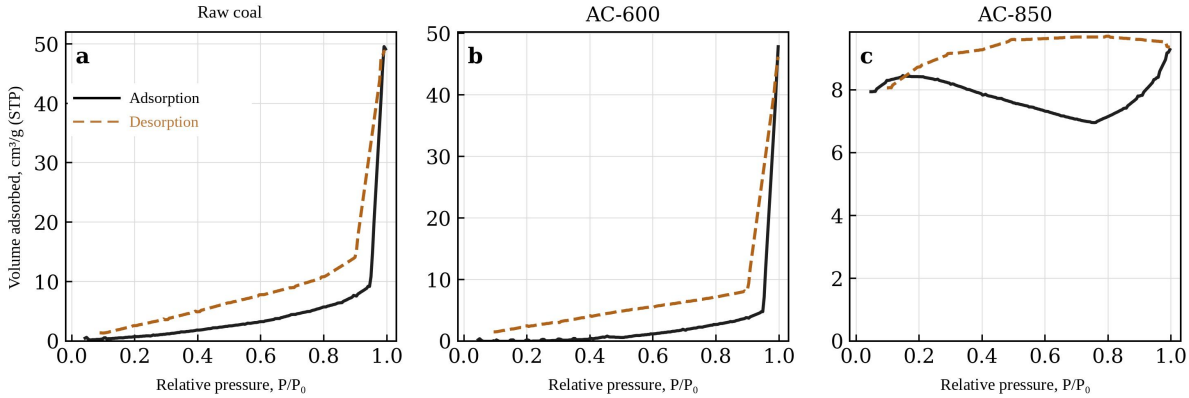


Figure 1 – Nitrogen adsorption–desorption isotherms at 77.35 K. Note the different ordinate scale of panel c

Two defects of the AC-850 isotherm must be stated. Its adsorption branch falls between P/P_0 = 0.20 and 0.75, which is physically impossible and points to an error in the free-space determination; the cold-zone volume recorded for this sample, 2.33515 cm^3, is 1.52 times that of the other two, and an error in this quantity produces exactly such a cumulative drift at higher pressures. Consequently no total pore volume can be assigned to AC-850 and only the low-pressure part of its isotherm is used below. The second defect is that the lowest measured point, P/P_0 = 0.053, already corresponds to 94 % of the plateau uptake: the micropore filling region itself was not sampled.

3.2. Textural parameters. Table 2 collects the DFT and BET results together with the width range over which each was computed.

Table 2 – Textural parameters; each value refers to the range stated in the same column

Parameter	Raw coal	AC-600	AC-850
Surface area (DFT), m2/g	12.142	6.781	33.704
Pore volume (DFT), cm3/g	0.059	0.048	0.0139
Distribution range, nm	0.71–25.1	0.97–18.0	0.74–5.53
Modal half-width, nm	2.59	7.66	1.66
Fitting error, %	6.864	1.717	0.089
Lower confidence limit, nm	0.708	0.966	0.739
Surface area (BET), m2/g	8.088	—	24.381
BET C constant	1.799	—	−36.725
BET correlation, r	0.9263	—	0.9935

AC-600 gives 6.781 m2/g, below the feedstock value, and its modal half-width has moved from 2.59 to 7.66 nm. AC-850 gives 33.704 m2/g with a modal half-width of 1.66 nm. The apparent fall of the AC-850 pore volume to 0.0139 cm3/g is not evidence of a smaller pore system: the distribution for this sample terminates at 5.53 nm, so everything wider is simply absent from the figure. For the same reason the mean width of 0.82 nm obtained from $S \approx 2V/w$ describes only the 0.74–5.53 nm interval.

© 2026 International Conference on Multidisciplinary Sciences and Innovations . All Rights Reserved.

A comparison restricted to that common interval is given in Table 3. It is the only quantitative comparison in this work that is free of range and kernel artefacts.

Table 3 – Raw coal and AC-850 over the common width range

Parameter (0.74–5.53 nm)	Raw coal	AC-850	Ratio
Pore volume, cm3/g	0.0083	0.0139	1.67
Surface area, m2/g	5.06	33.70	6.66

3.3. Pore size distribution. The distributions (Figure 2) show the qualitative difference directly. For the raw coal nothing is resolved below a half-width of 2.34 nm. For AC-850 the distribution begins at the lower confidence limit of the model, 0.739 nm, and at that very first point the cumulative volume is already 0.0112 cm^3/g and the cumulative surface 30.6 m^2/g — 80 % of the volume and 91 % of the surface. These fractions are not measured values but the residue that the model places in its first bin, and they show how much of the structure lies beyond what nitrogen at 77 K can resolve. AC-600 also shows a secondary peak near 1.8 nm, but it was computed with a different kernel after milder outgassing and is not compared quantitatively here.

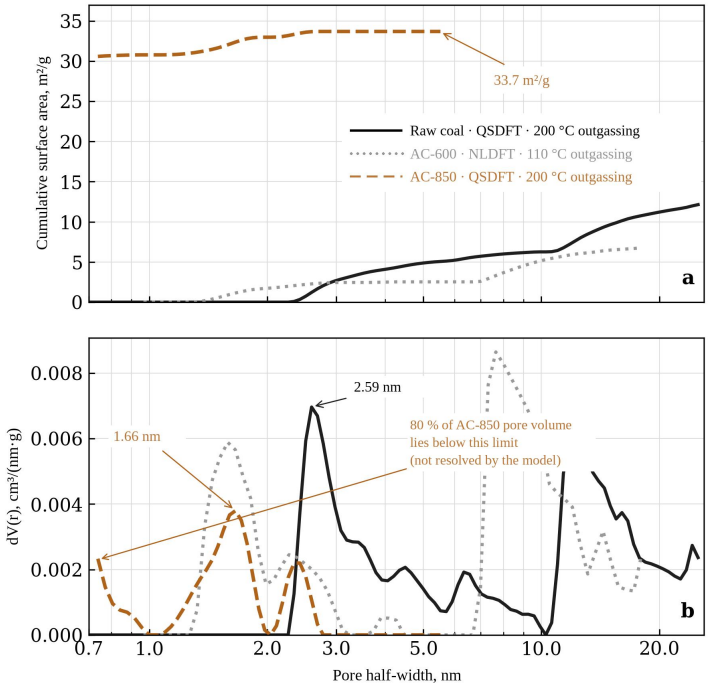


Figure 2 – Pore size distributions: (a) cumulative surface area; (b) differential distribution dV(r)

3.4. Composition. The EDS averages are given in Table 4. They are reported as an indication only: the determination is standardless and normalised, AC-850 was analysed at a single spot, and the silicon content falls from 1.87 to 0.12 wt.% on activation. That fall contradicts the mass balance, since mineral matter must be concentrated as carbon is burnt off; it therefore reflects the uneven distribution of mineral inclusions and the small number of spots rather than a real change. Only the sulphur figures, which are low and stable across all three samples at 0.23–0.43 wt.%, can be regarded as robust.

Table 4 – Mean spot composition by EDS, wt.% (indicative)

Sample	Spots	C	O	S	Si
Raw coal	5	81.39	15.91	0.24	1.87

© 2026 International Conference on Multidisciplinary Sciences and Innovations . All Rights Reserved.

Sample	Spots	C	O	S	Si
AC-600	3	87.32	11.94	0.43	n.d.
AC-850	1	77.84	21.75	0.23	0.12

4. Discussion

The experiment answers the question it was designed to answer: between 600 and 850 °C there is a qualitative threshold. One hour of steam treatment at 600 °C does not create micropores, it only widens the pores already present; the same treatment at 850 °C creates them. The direction of the result is expected from the kinetics of the carbon–steam reaction, whose rate at 600 °C is too low for appreciable burn-off within an hour [6, 7]. The contribution here is not the direction but the quantification of the threshold for this particular feedstock, and the practical consequence that raising the temperature is more effective than extending the time: at 600 °C the limitation is the reaction rate, not the duration.

One qualification of the mechanism should be made explicit. In both regimes the pyrolysis and the activation were carried out at the same temperature, so the design does not separate the two effects. Devolatilization of a bituminous coal continues well above 600 °C, and the AC-600 char may therefore still contain tars that block the pore mouths — an explanation that would coexist with, rather than replace, the kinetic one. A cleaner design would pyrolyse every sample at a single high temperature and vary only the activation temperature; this is the arrangement proposed for the next series.

The failure of the BET equation for both samples deserves comment because the two failures are opposite. For the raw coal C = 1.799, that is, the interaction is so weak that no monolayer forms. For AC-850 the intercept is negative and C = −36.725 while the correlation is high at 0.9935: over the interval used, 0.053–0.306, the micropores are already full, which is the classical situation described by the Rouquerol criteria [10]. The remedy is to move the interval to lower pressures — but in this measurement there are no lower points to move to. The two values, 1.799 and −36.725, thus record two opposite physical states, and they illustrate why a BET area for an activated carbon should never be quoted without C and r.

The reported 33.704 m2/g must be read as a lower bound for two independent reasons: the micropore filling region was not sampled, and 80 % of the volume falls at the confidence limit of the kernel. Nitrogen at 77 K is in any case diffusion-limited in narrow micropores, and carbon dioxide adsorption at 273 K is the recommended complement [9]. Against industrial activated carbons for water treatment, whose areas run to hundreds and often above a thousand square metres per gram [6], even a corrected value would remain low, and the most probable reason is insufficient burn-off: one hour at 850 °C has seeded the micropore structure but has not developed it. Burn-off itself was not measured, and without it the effect of temperature cannot be separated from the effect of the extent of reaction — this is the single most important quantity missing from the present series.

An internal consistency check supports the AC-850 result. A surface area of 33.704 m2/g corresponds to a nitrogen monolayer capacity of 7.74 cm3/g, and the plateau observed on the isotherm is about 8.4 cm3/g; the same calculation for the raw coal gives 2.79 cm3/g against an observed 1.2 cm3/g at P/P0 = 0.30. The activated sample is thus the internally consistent one, as its fitting error of 0.089 % against 6.864 % also indicates.

5. Conclusions

1. Temperature is the decisive parameter of the steam activation of Shargun coal. One hour at 600 °C does not form a micropore network: the surface area stays at or below the feedstock value and the modal half-width moves from 2.59 to 7.66 nm, that is, the existing pores merely widen.

© 2026 International Conference on Multidisciplinary Sciences and Innovations . All Rights Reserved.

2. The same treatment at 850 °C forms a microporous structure. The surface area reaches 33.704 m2/g and the modal half-width falls to 1.66 nm; uptake at P/P0 = 0.053 is 47.5 times that of the raw coal. Over the common range 0.74–5.53 nm the activated sample exceeds the feedstock by 1.67 times in pore volume and 6.7 times in surface area.

3. The BET equation is inapplicable to both samples for opposite reasons, C = 1.799 and C = −36.725. A BET area for an activated carbon should always be reported together with C and the correlation coefficient.

4. The value of 33.704 m2/g is a lower bound: the micropore filling region was not measured, and 80 % of the pore volume lies at the confidence limit of the model.

5. For the next stage: build the working regime around 850 °C; pyrolyse all samples at a single temperature and vary only the activation temperature; measure burn-off and yield at every point; extend the isotherm to relative pressures of 10−5 and add carbon dioxide adsorption at 273 K; and characterise all samples after the same outgassing regime (300 °C, at least 6 h) with the same QSDFT kernel.

References

1. Resolution of the President of the Republic of Uzbekistan “On measures for the development of renewable and hydrogen energy in the Republic of Uzbekistan”, No. PQ-5063. – Tashkent, 9 April 2021. – lex.uz.
2. Decree of the President of the Republic of Uzbekistan “On the Uzbekistan – 2030 Strategy”, No. PF-158. – Tashkent, 11 September 2023. – lex.uz.
3. Kang D., Kim J., Kim D., Kim S. The effect of water treatment processes on the performance of proton exchange membrane water electrolysis // Water. – 2026. – Vol. 18, No. 10. – Art. 1213. – DOI: 10.3390/w18101213.
4. Luukkonen T., Tolonen E.-T., Runtti H. et al. Removal of total organic carbon (TOC) residues from power plant make-up water by activated carbon // Journal of Water Process Engineering. – 2014. – Vol. 3. – P. 46–52. – DOI: 10.1016/j.jwpe.2014.08.005.
5. Salikhanova D., Usmonova Z., Sobirjonova S., Ubaydullaeva N., Karabayeva M. Obtainment of activated carbon by processing plum stones and using them in industrial wastewater purification // E3S Web of Conferences. – 2024. – Vol. 486. – Art. 01017. – DOI: 10.1051/e3sconf/202448601017.
6. Marsh H., Rodríguez-Reinoso F. Activated Carbon. – Amsterdam: Elsevier, 2006. – 536 p.
7. Xiong S., Lv F., Wang C. et al. Coal-based activated carbon prepared by H2O activation process for supercapacitors using response surface optimization method // Frontiers of Chemical Science and Engineering. – 2024. – Vol. 18. – Art. 63. – DOI: 10.1007/s11705-024-2422-4.
8. Zhang L., Zuo S. The significance of lignocellulosic raw materials on the pore structure of activated carbons prepared by steam activation // Molecules. – 2024. – Vol. 29, No. 13. – Art. 3197. – DOI: 10.3390/molecules29133197.
9. Thommes M., Kaneko K., Neimark A.V. et al. Physisorption of gases, with special reference to the evaluation of surface area and pore size distribution (IUPAC Technical Report) // Pure and Applied Chemistry. – 2015. – Vol. 87, No. 9–10. – P. 1051–1069. – DOI: 10.1515/pac-2014-1117.
10. Rouquerol J., Llewellyn P., Rouquerol F. Is the BET equation applicable to microporous adsorbents? // Studies in Surface Science and Catalysis. – 2007. – Vol. 160. – P. 49–56.
11. Neimark A.V., Lin Y., Ravikovitch P.I., Thommes M. Quenched solid density functional theory and pore size analysis of micro-mesoporous carbons // Carbon. – 2009. – Vol. 47, No. 7. – P. 1617–1628. – DOI: 10.1016/j.carbon.2009.01.050.
12. Landers J., Gor G.Y., Neimark A.V. Density functional theory methods for characterization of porous materials // Colloids and Surfaces A. – 2013. – Vol. 437. – P. 3–32. – DOI: 10.1016/j.colsurfa.2013.01.007.

© 2026 International Conference on Multidisciplinary Sciences and Innovations . All Rights Reserved.

13. Kwiatkowski M. An analysis of the textural properties of activated carbons obtained from biomass via the LBET, NLDFT and QSDFT methods // Scientific Reports. – 2024. – Vol. 14. – Art. 26472. – DOI: 10.1038/s41598-024-76297-x.
14. Anvarova I. Determination of the adsorption properties of activated carbon obtained from local raw materials for the regeneration of amine solutions used in natural gas treatment // Journal of Integrated Education and Research. – 2022. – Vol. 1, No. 6. – P. 90–93. (in Uzbek)